

## Chiral Tetranuclear $\mu_3$ -Alkoxo-Bridged Copper(II) Complex with 2 + 4 Cubane-Like $\text{Cu}_4\text{O}_4$ Core Framework and Ferromagnetic Ground State

Anja Burkhardt, Eike T. Spielberg, Helmar Görls, and Winfried Plass\*

Institut für Anorganische und Analytische Chemie, Friedrich-Schiller-Universität Jena, Carl-Zeiss-Promenade 10, 07745 Jena, Germany

Received September 10, 2007

The sugar-modified Schiff base ligand benzyl 2-deoxy-2-salicylideneamino- $\alpha$ -D-glucopyranoside  $\text{H}_2\text{L}$ , prepared by condensation of salicylaldehyde and the monomeric chitosan analogue benzyl 2-deoxy-2-amino- $\alpha$ -D-glucopyranoside, reacts with copper(II) acetate to form a self-assembled, alkoxo-bridged tetranuclear homoleptic copper(II) complex  $[\{\text{Cu}(\text{L})\}_4]$  (**4**) with  $\text{Cu}_4\text{O}_4$  heterocubane core. The chiral complex **4** crystallizes in the space group  $P2_12_12_1$ . The tetranuclear complex **4** is composed of two dinuclear  $\{\text{Cu}(\text{L})\}_2$  entities linked by the four  $\mu_3$ -bridging C-3 alkoxide oxygen atoms of the sugar backbone. The preorganization of the dimeric  $\{\text{Cu}(\text{L})\}_2$  entities is enforced by strong hydrogen bonds between the phenolate oxygen atom and the C-4 hydroxy group of the two constituting chiral monomeric building blocks. Therefore the  $\text{Cu}_4\text{O}_4$  core can be classified as a type I or 2 + 4 cubane. The chirality of the structure is confirmed by circular dichroism (CD) spectra, which reveal a significant dichroism associated with the copper centered transitions at around 600 nm. Temperature dependent magnetic susceptibility measurements indicate ferromagnetic exchange interactions in complex **4**. Fitting of the experimental data with a two  $J$  model based on the 2 + 4 topology ( $\hat{H} = -J_1(\hat{S}_1\hat{S}_3 + \hat{S}_2\hat{S}_4) - J_2(\hat{S}_1 + \hat{S}_3)(\hat{S}_2 + \hat{S}_4)$ ) leads to exchange coupling constants of  $J_1 = 64$  and  $J_2 = 4 \text{ cm}^{-1}$ . The observed ferromagnetic coupling can be attributed to the very small Cu–O–Cu bridging angles within the  $\text{Cu}_2\text{O}_2$  core of the constituting dimeric entities, which are a result of the conformational requirements introduced by the sugar backbone. **4** is not only the first example of an alkoxo-bridged tetranuclear copper(II) complex with  $\text{Cu}_4\text{O}_4$  core representing the 2 + 4 cubane class with ferromagnetic ground state but also a rare example for the class of molecules combining a ferromagnetic ground state with optical activity. The ferromagnetic  $S = 2$  ground state of **4** is confirmed by magnetization measurements and ESR spectroscopy.

### Introduction

High-nuclearity transition-metal complexes have been attracting continuous interest because of their relevance for multimetal active sites of metalloproteins<sup>1</sup> as well as their importance in the field of molecular magnetism.<sup>2,3</sup> Within the latter context recently particular interest arose in the combination of magnetic properties and chirality in one molecule, due to the observation of magnetochirality<sup>4</sup> which potentially contributes to the answer of the origin of

homochirality of life.<sup>5,6</sup> Over the years particular emphasis has been placed on copper because of its central role in biology.<sup>7,8</sup> Moreover, also from a magnetostructural point of view multicopper complexes have been extensively studied both with experimental and theoretical approaches. In this context recently the tetranuclear cubane-like copper(II) complexes have received special attention.<sup>9,10</sup> Nevertheless,

\* To whom correspondence should be addressed. E-mail: sekr.plass@uni-jena.de.

- (1) Holm, R. H.; Kennepohl, P.; Solomon, E. I. *Chem. Rev.* **1996**, *96*, 2239–2314.
- (2) Kahn, O. *Molecular Magnetism*; VCH: Weinheim, 1993.
- (3) Winpenny, R. E. P. *Adv. Inorg. Chem.* **2001**, *52*, 1–111.
- (4) Rikken, G. L. J. A.; Raupach, E. *Nature* **1997**, *390*, 493–494.

- (5) Barron, L. D. *Science* **1994**, *266*, 1491–1492.
- (6) Rikken, G. L. J. A.; Raupach, E. *Nature* **2000**, *405*, 932–935.
- (7) Solomon, E. I.; Sundaram, U. M.; Machonkin, T. E. *Chem. Rev.* **1996**, *96*, 2563–2605.
- (8) *Handbook of Metalloproteins*; Messerschmidt, A., Huber, R., Poulos, T., Wieghardt, K., Eds.; John Wiley & Sons: Chichester, 2001; Vol. 2.
- (9) Mukherjee, A.; Raghunathan, R.; Saha, M. K.; Nethaji, M.; Ramasesha, S.; Chakravarty, A. R. *Chem. Eur. J.* **2005**, *11*, 3087–3096.
- (10) Tercero, J.; Ruiz, E.; Alvarez, S.; Rodríguez-Forteza, A.; Alemany, P. *J. Mater. Chem.* **2006**, *16*, 2729–2735.

although chiral ligands have been employed in the synthesis, homochiral examples of such cubane-like copper(II) complexes have not yet been reported.<sup>11–14</sup>

One method to construct polynuclear transition-metal complexes is self-assembly of coordinatively unsaturated mononuclear units obtained from polydentate ligands. Because of their polyfunctionality carbohydrates are suitable chelate ligands which can utilize their vicinal functional groups to form polynuclear complexes with several transition-metal ions.<sup>15–17</sup> Moreover, sugars not only combine interesting properties like a stable chiral scaffold and the ability to support supramolecular arrangements via hydrogen bonding but also allow for a broad variety of derivatizations of their functional groups. Well-known modification strategies to introduce additional donor groups into the sugar backbone are *N*-glycosylation with polyamines<sup>18–20</sup> and nucleophilic substitution of bromoethyl-*O*-glycosides.<sup>21,22</sup> TEMPO oxidation of the secondary hydroxyl group at C-6 results in uronic acids. The corresponding carbohydrate-derived salicylidene hydrazides obtained via a three-step synthesis support mononuclear dioxovanadium(V) complexes.<sup>23</sup> Alternatively, the condensation reaction of amino saccharides and carbonyl components yields tridentate Schiff base ligands.<sup>24–26</sup> These imino ligands are based on either C-1 or C-6 amino functionalized carbohydrate fragments and yield mono- and dinuclear VO<sub>2</sub><sup>+</sup>, MoO<sub>2</sub><sup>2+</sup>, and UO<sub>2</sub><sup>2+</sup> complexes<sup>26,27</sup> as well as several copper(II) complexes with varying nuclearity and architecture. In the latter case the structure of the central Cu<sub>*n*</sub> unit (*n* = 2, 3, 4) can be influenced by the positions of the chelating donor atoms at the sugar moiety. In particular, 6-imino- or 6-ketoenamine-glucopyranose derivatives form six-membered chelate rings leading to alkoxo-acetato-bridged trinuclear complexes, whereas ligands containing 1- or 2-imino-glucopyranose,

1-imino-sorbitol, or 5-ketoenamine-glucufuranose units yield di- or tetranuclear alkoxo-bridged copper(II) compounds with five-membered chelate rings.<sup>28–35</sup>

The present work explores the scarce coordination chemistry of 2-aminoglucose based Schiff base ligands with the aim to generate chiral magnetic copper(II) complexes. Herein, we report on the synthesis of the first chiral tetranuclear cubane-like copper(II) complex with a ferromagnetic ground state by utilizing a 2-aminoglucose-based Schiff base ligand.

## Experimental Section

**Materials.** The precursor ligand benzyl 2-acetamido-2-deoxy- $\alpha$ -D-glucopyranoside (**1**) was prepared from *N*-acetyl- $\alpha$ -D-glucopyranosamine according to a published procedure.<sup>36</sup> All other chemicals were purchased from commercial suppliers and applied as received.

**Physical Measurements.** Melting points are given uncorrected and were performed with a BÜCHI melting point apparatus type B-540. Thermogravimetric analyses (TGA) were performed on powdered samples with a NETZSCH STA409PC Luxx apparatus under constant flow of nitrogen ranging from room temperature up to 1000 °C with a heating rate of 1 °C/min. Infrared and Raman spectra were carried out on a BRUKER IFS 55 EQUINOX spectrometer. <sup>1</sup>H, <sup>13</sup>C NMR, <sup>1</sup>H{<sup>1</sup>H} COSY, and <sup>1</sup>H{<sup>13</sup>C} heteronuclear correlation NMR spectra were recorded on BRUKER AVANCE 400 and 200 MHz spectrometers. UV/vis spectra were recorded on a VARIAN CARY 5000 UV/vis/NIR spectrometer. Circular dichroism (CD) spectra were determined on a JASCO J-810 CD spectrometer. Mass spectra were performed on a BRUKER MAT SSQ 710 spectrometer. Elemental analyses were acquired by use of LECO CHNS/932 and VARIO EL III elemental analyzers. X-Band (9 GHz) electron spin resonance (ESR) measurements were performed on powdered samples at room temperature and 77 K using a BRUKER ESP 300E spectrometer. Magnetic susceptibilities were determined for powdered samples at an applied magnetic field of 2 kOe using a Quantum Design MPMSR-5S SQUID magnetometer from Quantum Design in the range from 300 to 2 K (for details see refs 37 and 38). The diamagnetic corrections were estimated according to Pascal's constants.

**Synthesis of Benzyl 2-Deoxy-2-salicylideneamino- $\alpha$ -D-glucopyranoside (H<sub>2</sub>L) (**3**).** Benzyl 2-acetamido-2-deoxy- $\alpha$ -D-glucopyranoside (**1**; 1.00 g, 3.21 mmol) and potassium hydroxide (7.02 g, 125.11 mmol) were heated under reflux overnight in 25 mL of ethanol. After cooling to room temperature the orange mixture was diluted with 50 mL of ethanol and neutralized with aqueous HCl. The precipitated potassium chloride was separated via centrifugation, and the supernatant was reduced to 10 mL in volume. After

- (11) Laurent, J.-P.; Bonnet, J.-J.; Nepveu, F.; Astheimer, H.; Walz, L.; Haase, W. *J. Chem. Soc., Dalton Trans.* **1982**, 2433–2438.
- (12) Walz, L.; Paulus, H.; Haase, W.; Langhof, H.; Nepveu, F. *J. Chem. Soc., Dalton Trans.* **1983**, 657–664.
- (13) Astheimer, H.; Nepveu, F.; Walz, L.; Haase, W. *J. Chem. Soc. Dalton Trans.* **1985**, 315–320.
- (14) Wegner, R.; Gottschaldt, M.; Görls, H.; Jäger, E.-G.; Klemm, D. *Chem. Eur. J.* **2001**, 7, 2143–2157.
- (15) Klüfers, P.; Kunte, T. *Angew. Chem., Int. Ed.* **2001**, 40, 4210–4212.
- (16) Klüfers, P.; Kunte, T. *Eur. J. Inorg. Chem.* **2002**, 1285–1289.
- (17) Klüfers, P.; Krotz, O.; Ossberger, M. *Eur. J. Inorg. Chem.* **2002**, 1919–1923.
- (18) Yano, S. *Coord. Chem. Rev.* **1988**, 92, 113–156.
- (19) Tanase, T.; Nakagoshi, M.; Teratani, A.; Kato, M.; Yamamoto, Y.; Yano, S. *Inorg. Chem.* **1994**, 33, 5–6.
- (20) Tanase, T.; Inukai, H.; Onaka, T.; Kato, M.; Yano, S.; Lippard, S. J. *Inorg. Chem.* **2001**, 40, 3943–3953.
- (21) Storr, T.; Obata, M.; Fisher, C. L.; Bayly, S. R.; Green, D. E.; Brudzińska, I.; Mikata, Y.; Patrick, B. O.; Adam, M. J.; Yano, S.; Orvig, C. *Chem. Eur. J.* **2005**, 11, 195–203.
- (22) Mikata, Y.; Sugai, Y.; Obata, M.; Harada, M.; Yano, S. *Inorg. Chem.* **2006**, 45, 1543–1551.
- (23) Becher, J.; Seidel, I.; Plass, W.; Klemm, D. *Tetrahedron* **2006**, 62, 5675–5681.
- (24) Irvine, J. C.; Earl, J. C. *J. Chem. Soc.* **1922**, 121, 2376–2381.
- (25) Cucciolo, M. E.; Del Litto, R.; Roviello, G.; Ruffo, F. *J. Mol. Catal. A: Chem.* **2005**, 236, 176–181.
- (26) Sah, A. K.; Rao, C. P.; Saarenketo, P. K.; Wegelius, E. K.; Kolehmainen, E.; Rissanen, K. *Eur. J. Inorg. Chem.* **2001**, 11, 2773–2781.
- (27) Zhao, J.; Zhou, X.; Santos, A. M.; Herdtweck, E.; Romão, C. C.; Kühn, F. E. *Dalton Trans.* **2003**, 3736–3742.

- (28) Wegner, R.; Gottschaldt, M.; Görls, H.; Jäger, E.-G.; Klemm, D. *Angew. Chem., Int. Ed.* **2000**, 39, 595–599.
- (29) Fragoso, A.; Kahn, M. L.; Castiñeiras, A.; Sutter, J.-P.; Kahn, O.; Cao, R. *Chem. Commun.* **2000**, 1547–1548.
- (30) Sah, A. K.; Rao, C. P.; Saarenketo, P. K.; Rissanen, K.; van Albada, G. A.; Reedijk, J. *Chem. Lett.* **2002**, 31, 348–349.
- (31) Sah, A. K.; Tanase, T. *Chem. Commun.* **2005**, 5980–5981.
- (32) Sah, A. K.; Kato, M.; Tanase, T. *Chem. Commun.* **2005**, 675–677.
- (33) Sah, A. K.; Tanase, T.; Mikuriya, M. *Inorg. Chem.* **2006**, 45, 2083–2092.
- (34) Burkhardt, A.; Buchholz, A.; Görls, H.; Plass, W. *Eur. J. Inorg. Chem.* **2006**, 3400–3406.
- (35) Roth, A.; Becher, J.; Herrmann, C.; Görls, H.; Vaughan, G.; Reiher, M.; Klemm, D.; Plass, W. *Inorg. Chem.* **2006**, 45, 10066–10076.
- (36) Györgydeák, Z. *Liebigs Ann. Chem.* **1991**, 1291–1300.
- (37) Plass, W. *Angew. Chem., Int. Ed. Engl.* **1996**, 35, 627–631.
- (38) Plass, W. *Inorg. Chem.* **1997**, 36, 2200–2205.

addition of sodium bicarbonate (344 mg, 4.09 mmol) and salicylaldehyde (436  $\mu\text{L}$ , 4.09 mmol) the mixture was stirred for 2.5 h at room temperature. The solvent was completely removed under reduced pressure, and the brownish residue was dissolved in a mixture of 25 mL of chloroform and 15 mL of water. The water layer was extracted twice with 5 mL of chloroform. The combined organic layers were dried over sodium sulfate, filtered, and concentrated in vacuo to a volume of 10 mL. The viscous solution was dropped into 120 mL of *n*-hexane yielding the product as a yellow precipitate. After reprecipitation in *n*-hexane the product was collected by filtration, washed with a small amount of *n*-hexane, and finally dried in air. Yield: 672 mg (56%). Mp: 78–79 °C. Anal. Calcd for  $\text{C}_{20}\text{H}_{23}\text{NO}_6$  (373.39): C, 64.3; H, 6.2; N, 3.8. Found: C, 63.1; H, 6.2; N, 3.6. IR (KBr,  $\text{cm}^{-1}$ ): 3392 br ( $\nu$  O–H), 2922 (s), 1632 vs ( $\nu$  C=N), 1581 w, 1497 s, 1457 s, 1418 w, 1340 w, 1280 s, 1211 w, 1141 s, 1096 s, 1037 vs, 902 w, 795 w, 759 s, 737 s, 698 s, 542 w.  $^1\text{H}$  NMR (400 MHz, DMSO- $d_6$ , 25 °C, ppm): 3.21–3.24 (m, 1H, H4), 3.27 (dd,  $J_{21} = 3.7$  Hz,  $J_{23} = 9.9$  Hz, 1H, H2), 3.52–3.62 (m, 2H, H5 and H6a), 3.67–3.74 (m, 2H, H3 and H6b), 4.47 and 4.74 (2d,  $J_{7a7b} = 12.4$  Hz, each 1H, H7a, H7b), 4.62 (t,  $J_{6\text{OH}} = 5.5$  Hz, 1H, OH6), 4.88 (d,  $J_{12} = 3.7$  Hz, 1H, H1), 5.08 (d,  $J_{4\text{OH}} = 5.5$  Hz, 1H, OH4), 5.13 (d,  $J_{3\text{OH}} = 5.5$  Hz, 1H, OH3), 6.85–6.89 and 7.24–7.45 (2m, 9H, Ph), 8.50 (s, 1H, H14), 14.00 (s, 1H, OH Ph).  $^{13}\text{C}$  NMR (50 MHz, DMSO- $d_6$ , 25 °C, ppm): 60.9 (C6), 67.9 (C7), 70.3 (C4), 71.3 (C3), 71.7 (C2), 73.4 (C5), 97.4 (C1), 116.7, 118.1, 118.6 (C15, C17, C19), 127.4, 128.2 (Ph), 131.7, 132.4 (C16, C18), 137.9 (C8), 161.4 (C20), 167.2 (C14). ESI-MS:  $m/z$  374 (20%)  $[(\text{H}_2\text{L}) + \text{H}]^+$ , 396 (100%)  $[(\text{H}_2\text{L}) + \text{Na}]^+$ .

**Synthesis of  $[\{\text{Cu}(\text{L})\}_4]$  (**4**).** A suspension of  $\text{Cu}(\text{CH}_3\text{COO})_2 \cdot \text{H}_2\text{O}$  (43 mg, 0.22 mmol) in 2 mL of acetonitrile was added to a solution of **3** (80 mg, 0.21 mmol) in 4 mL of acetonitrile at room temperature. After approximately 1 min of vigorous stirring a pale blue solid precipitated which was immediately dissolved by addition of 3 mL of methanol. After 2 weeks slow evaporation complex **4** gave blue crystals of  $4 \cdot 2\text{H}_2\text{O} \cdot 0.75\text{MeOH} \cdot 2.25\text{CH}_3\text{CN}$  which were suitable for X-ray diffraction. The crystals were isolated, washed with a small amount of methanol, and dried in air. Yield: 63 mg (66%). Decomposition interval = 255–278 °C. Anal. Calcd for  $\text{C}_{80}\text{H}_{88}\text{O}_{26}\text{N}_4\text{Cu}_4$  (1775.75): C, 54.1; H, 5.0; N, 3.2. Found: C, 54.0; H, 5.1; N, 2.9. IR (KBr,  $\text{cm}^{-1}$ ): 3436 br ( $\nu$  O–H), 3259 br ( $\nu$  O–H), 2899 s, 1637 vs ( $\nu$  C=N), 1603 s, 1543 s, 1472 w, 1452 vs, 1400 w, 1380 w, 1342 w, 1320 s, 1299 s, 1257 w, 1201 s, 1155 s, 1125 s, 1106 s, 1085 s, 1055 vs, 1024 vs, 979 s, 913 w, 895 w, 842 w, 811 w, 757 s, 740 w, 700 w, 623 w, 611 w, 586 w, 544 w, 520 w. Raman (solid,  $\text{cm}^{-1}$ ): 3054 s ( $\nu$  C–H arom.), 2892 w, 1636 vs ( $\nu$  C=N), 1604 w, 1542 vs, 1472 w, 1453 s, 1346 vs, 1255 w, 1211 w, 1155 w, 1086 w, 1036 w, 1003 s, 913 w, 895 w, 812 w, 621 w. UV/vis ( $\text{CHCl}_3$ ,  $\lambda_{\text{max}}/\text{nm}$  ( $\epsilon/\text{L mol}^{-1} \text{cm}^{-1}$ ): 272 (6380); 280 (6960); 363 (2320); 597 (50). ESI-MS:  $m/z$  870 (36%)  $[\{\text{Cu}(\text{L})\}_2 + \text{H}]^+$ , 892 (100%)  $[\{\text{Cu}(\text{L})\}_2 + \text{Na}]^+$ , 1327 (10%)  $[\{\text{Cu}(\text{L})\}_3 + \text{Na}]^+$ , 1740 (10%)  $[\{\text{Cu}(\text{L})\}_4 + \text{H}]^+$ , 1762 (66%)  $[\{\text{Cu}(\text{L})\}_4 + \text{Na}]^+$ .

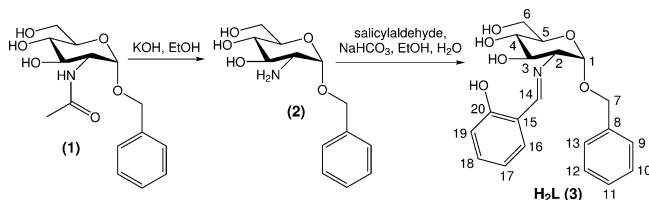
**X-ray Structure Determinations.** Crystallization of complex **4** from a mixture of acetonitrile and methanol afforded blue prismatic crystals of  $4 \cdot 2\text{H}_2\text{O} \cdot 0.75\text{MeOH} \cdot 2.25\text{CH}_3\text{CN}$  suitable for X-ray measurements. Single crystals were selected while still covered with mother liquor under a polarizing microscope and fixed on fine glass fibers. X-ray measurements were recorded on a Nonius Kappa CCD diffractometer using graphite monochromated Mo K $\alpha$  radiation ( $\lambda = 0.1073$  Å). Data were corrected for Lorentz and polarization effects but not for absorption. Details of the data collection and refinement procedure are summarized in Table 1. The structure was solved by direct methods (SHELXS) and was full-matrix least-squares refined against  $F^2$  (SHELXL) utilizing the

**Table 1.** Crystallographic Data and Structure Refinement Parameters for  $4 \cdot 2\text{H}_2\text{O} \cdot 0.75\text{MeOH} \cdot 2.25\text{CH}_3\text{CN}$

formula	$\text{C}_{85.25}\text{H}_{93.75}\text{Cu}_4\text{N}_{6.25}\text{O}_{26.75}$
fw ( $\text{g mol}^{-1}$ )	1888.08
$T$ (K)	183(2)
crystal size ( $\text{mm}^3$ )	$0.6 \times 0.5 \times 0.5$
crystal system	orthorhombic
space group	$P2_12_12_1$
$a$ (Å)	17.353(4)
$b$ (Å)	18.353(4)
$c$ (Å)	27.782(6)
$V$ (Å $^3$ )	8848(3)
$Z$	4
$\rho_{\text{calcd}}$ ( $\text{g cm}^{-3}$ )	1.417
$\mu$ ( $\text{mm}^{-1}$ )	1.029
$\theta$ range (deg)	2.34–27.49
measured data	61183
unique data ( $R_{\text{int}}$ )	20230 (0.0711)
data with $I > 2\sigma(I)$	12867
no. of parameters	1102
goodness of fit $s^a$ on $F^2$	0.996
$R1^b$ ( $I > 2\sigma(I)$ )	0.0509
$wR2^c$ (all data)	0.1198
flack parameter	–0.007(8)
residual density ( $\text{e Å}^{-3}$ )	–0.477/0.557

$^a S = \{\sum[w(F_o^2 - F_c^2)^2]/(N_r - N_p)\}^{1/2}$ .  $^b R1 = \sum||F_o| - F_c||/\sum|F_o|$ .  $^c wR2 = \{\sum[w(F_o^2 - F_c^2)^2]/\sum[w(F_o^2)^2]\}^{1/2}$  with  $w^{-1} = \sigma^2(F_o^2) + (0.06P)^2$  and  $P = (1/3)[\max(0, F_o^2) + 2F_c^2]$ .

**Scheme 1.** Reaction Scheme for the Synthesis of Ligand  $\text{H}_2\text{L}$  (**3**)



program package SHELX-97.<sup>39</sup> For all non-hydrogen atoms anisotropic thermal parameters were used, except for the disordered phenyl ring of the protecting group at the ligand fragment of the  $\{\text{Cu}(\text{L})\}$  building block at Cu1. Hydrogen atoms were calculated and treated as riding atoms with fixed thermal parameters. The crystallographic positions located for acetonitrile and methanol solvent molecules were found to be only partially occupied and were refined with an occupancy factor of 0.75. The program XP (Siemens Analytical X-ray Instruments, Inc.) was used for structure representations. Crystallographic data can be obtained free of charge as CCDC-657012 from the Cambridge Crystallographic Data Centre via [www.ccdc.cam.ac.uk/data\\_request/cif](http://www.ccdc.cam.ac.uk/data_request/cif) or 12 Union Road, Cambridge CB2 1EZ, U.K.

## Results and Discussion

**Synthesis and Characterization.** Utilizing the sugar precursor benzyl 2-acetamido-2-deoxy- $\alpha$ -D-glucopyranoside (**1**) the Schiff base ligand  $\text{H}_2\text{L}$  (**3**) was prepared by a two-step synthesis as depicted in Scheme 1. After alkaline deacetylation of the starting material benzyl 2-acetamido-2-deoxy- $\alpha$ -D-glucopyranoside (**1**)<sup>36</sup> the resulting amino sugar (**2**) was converted to  $\text{H}_2\text{L}$  (**3**) without further purification by condensation with salicylaldehyde in a methanol/water mixture. The prepared Schiff base ligand **3** was characterized by IR, NMR, and ESI-MS studies as well as elemental analysis. In the IR spectrum of **3** the stretching vibration

(39) Sheldrick, G. M. *SHELX-97*; University of Göttingen: Göttingen, Germany, 1997.



associated with the imino group is found at  $1632\text{ cm}^{-1}$ . The corresponding  $^1\text{H}$  and  $^{13}\text{C}$  NMR resonances of the imino group are observed at 8.50 and 167.2 ppm, respectively. The doublet observed at 4.88 ppm in the  $^1\text{H}$  NMR spectrum with  $J_{12} = 3.7\text{ Hz}$  originates from the proton on C-1 of the sugar framework indicating the exclusive presence of the  $\alpha$ -anomer of the D-glucose unit.

The tetranuclear complex  $[\{\text{Cu}(\text{L})\}_4]$  (**4**) was prepared by addition of copper(II) acetate to a solution of  $\text{H}_2\text{L}$  (**3**) in a 1:1 molar ratio in acetonitrile solution at room temperature. After a few minutes a pale blue solid precipitated which redissolved immediately after the addition of methanol. **4** was obtained as blue prisms after slow evaporation of the solvent from the mother liquor.

The obtained crystals contain two water molecules per tetrameric copper complex and additional methanol and acetonitrile molecules of crystallization (see Experimental Section). Upon drying in air the crystals lose their acetonitrile and methanol molecules of crystallization which is evident from the elemental analysis leading to the formula  $[\{\text{Cu}(\text{L})\}_4] \cdot 2\text{H}_2\text{O}$  for the isolated complex ( $\mathbf{4} \cdot 2\text{H}_2\text{O}$ ). TGA of such an air-dried sample of complex  $\mathbf{4} \cdot 2\text{H}_2\text{O}$  reveals a weight loss of about 2% up to the decomposition starting at 255 K which can be attributed to the removal of the two molecules of water per tetrameric copper complex **4**.

UV/vis and CD spectra were recorded at room temperature for chloroform solutions of  $[\{\text{Cu}(\text{L})\}_4] \cdot 2\text{H}_2\text{O}$  ( $\mathbf{4} \cdot 2\text{H}_2\text{O}$ ) (see Figure 1). The electronic absorption studies show two charge transfer transition bands at 278 and 360 nm and an additional d–d transition band at around 600 nm. Significant dichroism is observed for all electronic absorptions. This particularly holds for the range between 500 and 650 nm which is associated with the copper(II) centers as evident by the comparison with the UV/vis absorption spectrum given in Figure 1. Consequently, the electronic absorptions at the copper centers are sensitive to the polarization of light. This clearly shows that the ligand imposed chirality is transferred to the magnetic center.

**Structure Description.** The molecular structure of  $[\{\text{Cu}(\text{L})\}_4]$  (**4**) is shown in Figure 2. Complex **4** crystallizes in the orthorhombic space group  $P2_12_12_1$  consistent with the exclusive presence of solely one enantiomeric form, which is in accordance with the CD spectra for solutions of **4** and

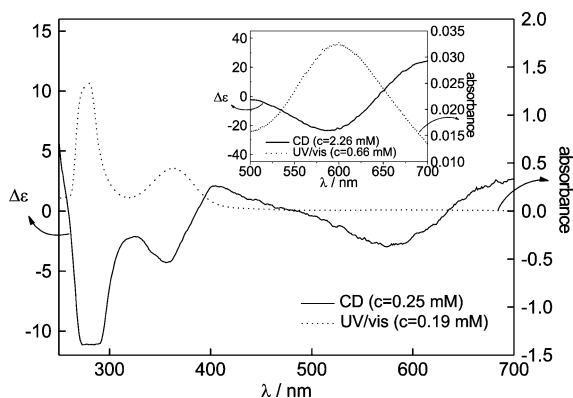


**Figure 1.** UV/vis (dotted lines) and CD spectra (solid lines) for  $[\{\text{Cu}(\text{L})\}_4] \cdot 2\text{H}_2\text{O}$  ( $\mathbf{4} \cdot 2\text{H}_2\text{O}$ ) in  $\text{CHCl}_3$  solutions at room temperature.

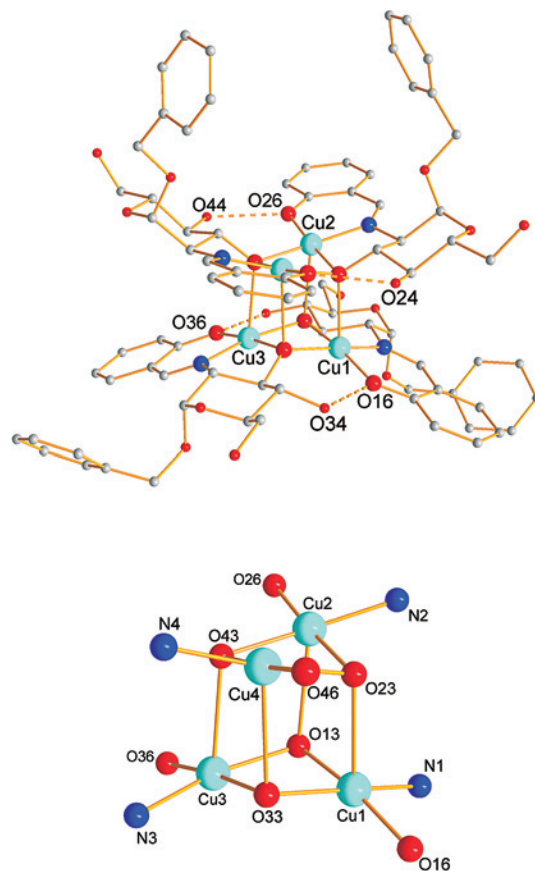


**Figure 2.** Molecular structure of  $[\{\text{Cu}(\text{L})\}_4]$  (**4**) in crystals of  $\mathbf{4} \cdot 2\text{H}_2\text{O} \cdot 0.75\text{MeOH} \cdot 2.25\text{CH}_3\text{CN}$ . Solvent molecules and hydrogen atoms are omitted for clarity. (top) Molecule including intramolecular hydrogen bonds indicated by dashed lines. Pertinent distances:  $\text{O14} \cdots \text{O36}$  263.3(4),  $\text{O24} \cdots \text{O46}$  258.6(4),  $\text{O44} \cdots \text{O26}$  259.2(4), and  $\text{O34} \cdots \text{O16}$  263.3(4) pm. (bottom) Representation of the  $\text{Cu}_4\text{O}_4$  core of **4** with the coordination environment of the copper(II) centers.

the NMR spectra of the constituting Schiff base ligand. The neutral complex **4** cocrystallized with two water molecules and additional more loosely associated solvent molecules of methanol and acetonitrile, which was found to be consistent with elemental analysis and TGA data. Selected bond lengths and angles as well as interatomic distances are summarized in Table 2.

All copper(II) centers are penta-coordinated with an  $\text{NO}_4$  donor set. The coordination environment is best described as square-pyramidal with the basal plane established by the phenolate oxygen atom of the salicylidene fragment, the C-2 imino nitrogen atom, and the C-3 alkoxide oxygen atom of the monosaccharide unit of one Schiff base ligand as well as an additional C-3 alkoxide oxygen atom of a second complex moiety. The apical position is occupied by a C-3 alkoxide oxygen atom of a third complex molecule at a rather long donor distance (vide infra). The donor atoms of all basal coordination planes deviate by less than 4 pm from the corresponding mean planes with the related copper(II) centers only slightly displaced toward the apical ligand (7–15 pm).

By a self-assembly process four chiral building blocks  $\{\text{Cu}(\text{L})\}$  form the tetranuclear complex **4** with a cubane-like  $\text{Cu}_4\text{O}_4$  central core. The vertices of the cube are alternately occupied by four copper(II) and four C-3 alkoxide oxygen atoms, leading to two interlocked distorted

**Table 2.** Selected Bond Lengths and Interatomic Distances (pm) and Bond Angles (deg) for  $[\{\text{Cu}(\text{L})\}_4]$  (**4**)

Distances			
Cu1–N1	194.4(3)	Cu2–N2	193.6(3)
Cu1–O13	198.2(3)	Cu2–O13	251.6(3)
Cu1–O16	189.1(3)	Cu2–O23	200.7(3)
Cu1–O23	241.3(3)	Cu2–O26	189.6(3)
Cu1–O33	196.4(2)	Cu2–O43	198.4(3)
Cu3–N3	193.5(3)	Cu4–N4	192.1(3)
Cu3–O13	198.1(2)	Cu4–O23	198.1(3)
Cu3–O33	198.0(3)	Cu4–O33	256.6(3)
Cu3–O36	189.2(3)	Cu4–O43	199.9(2)
Cu3–O43	245.0(3)	Cu4–O46	190.2(3)
Cu1...Cu2	338.32(8)	Cu2...Cu3	350.52(8)
Cu1...Cu3	289.32(8)	Cu2...Cu4	281.52(8)
Cu1...Cu4	348.56(8)	Cu3...Cu4	341.51(8)

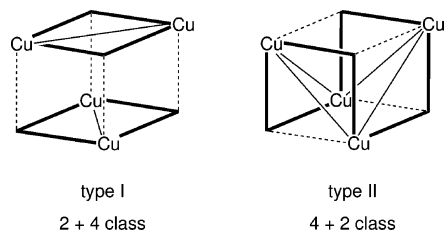
Angles			
Cu1–O13–Cu2	96.84(9)	Cu2–O13–Cu3	101.75(9)
Cu1–O13–Cu3	93.81(10)	Cu2–O23–Cu4	89.79(10)
Cu1–O23–Cu2	99.46(10)	Cu2–O43–Cu3	103.97(10)
Cu1–O23–Cu4	104.55(10)	Cu2–O43–Cu4	89.97(10)
Cu1–O33–Cu4	99.73(9)	Cu3–O33–Cu4	96.53(9)
Cu1–O33–Cu3	94.39(9)	Cu3–O43–Cu4	99.79(10)

tetrahedra of copper and oxygen atoms. Consequently, three copper(II) centers are linked in  $\mu_3$ -bridging fashion by a C-3 oxygen atom of the sugar backbone. The  $\mu_3$ -bridging oxygen atoms are deprotonated, affording a dianionic ligand fragment and finally complex **4** as a neutral species. Each Schiff base ligand **3** acts as a tridentate ligand for one copper(II) ion leading to five- and six-membered chelate rings with bite angles of 85 and 93°, respectively. The oxygen atoms at C-4 and C-6 of the sugar backbone remain protonated. Each monosaccharide unit adopts the more stable  ${}^4\text{C}_1$  chair conformation.

According to the  $\text{Cu}i\text{--O}i3$  bond lengths ( $i$  is the running number of the constituting  $\{\text{Cu}i(\text{L})\}$  moieties) the  $\text{Cu}_4\text{O}_4$  core structure should be rather described as composed of two dimeric  $\text{Cu}_2\text{O}_2$  units with short  $\text{Cu--O}$  bonds within the dimeric units (196–201 pm) and long  $\text{Cu--O}$  bonds between them (241–257 pm). The two resulting dimeric units  $\text{Cu1Cu3}$  and  $\text{Cu2Cu4}$  are constituted by the respective copper-ligand moieties. Each dimeric unit is additionally stabilized by two strong hydrogen bonds with an  $\text{O}\cdots\text{O}$  distance of about 260 pm between the phenolate oxygen atom  $\text{O}i6$  and the hydroxy group ( $\text{O}i4$ ) at C-4 of the sugar backbone from the supporting ligands **3** (see Figure 2). As a consequence of the stereochemistry of the sugar backbone, with  $\text{Ni--C}i\text{O}2\text{--C}i\text{O}3\text{--O}i3$  torsion angles in the range of 48–50°, these hydrogen bonds lead to the nonplanarity of the  $\text{Cu}_2\text{O}_2$  core fragment of the dimeric units. The dihedral angles between the  $\text{CuO}_2$  planes of the resulting butterfly structures of the dimeric units  $\text{Cu1Cu3}$  and  $\text{Cu2Cu4}$  are 150.7 and 159.8°, respectively. Hence, this leads to  $\text{Cu}i\text{--O}i3\text{--C}uj$  bond angles at the bridging oxygen atoms within the dimeric units  $\text{Cu1Cu3}$  and  $\text{Cu2Cu4}$  in the range between 89.8 and 94.4° (cf. Table 2), which are by far the smallest angles observed for alkoxo-bridged compounds with a  $\text{Cu}_2\text{O}_2$  core fragment.<sup>40–65</sup>

(40) Bertrand, J. A.; Fujita, E.; Eller, P. G. *Inorg. Chim. Acta* **1974**, *13*, 2067–2071.

(41) Bertrand, J. A.; Kirkwood, C. E. *Inorg. Chim. Acta* **1972**, *6*, 248–252.

**Scheme 2.** Classification of Tetranuclear Cubane Copper Complexes According to the  $\text{Cu--O}$  and  $\text{Cu}\cdots\text{Cu}$  Distances of the Central  $\text{Cu}_4\text{O}_4$  Core<sup>a</sup>

<sup>a</sup> See text. Thick lines represent short and broken lines long  $\text{Cu--O}$  distances. Short  $\text{Cu}\cdots\text{Cu}$  distances are indicated by a connecting line.

Compounds with a  $\text{Cu}_4\text{O}_4$  core structure have been classified in literature according their atomic distances within the core structure, namely, the  $\text{Cu--O}$  and  $\text{Cu}\cdots\text{Cu}$  distances.<sup>10,65–67</sup> The structures known to date almost exclusively fall into two classes, which can be denoted according their number of short and long  $\text{Cu}\cdots\text{Cu}$  distances within the  $\text{Cu}_4\text{O}_4$  core as 2 + 4 class (or type I) and 4 + 2 class (or type II) as depicted in Scheme 2, with the latter being by far the more common of the two cases. Besides these two

(42) Bertrand, J. A.; Kelley, J. A. *Inorg. Chim. Acta* **1970**, *4*, 203–209.

(43) Curtis, N. F.; Einstein, F. W. B.; Morgan, K. R.; Willis, A. C. *Inorg. Chim. Acta* **1985**, *24*, 2026–2032.

(44) Drillon, M.; Grand, A.; Rey, P. *Inorg. Chim. Acta* **1990**, *29*, 771–774.

(45) Handa, M.; Idehara, T.; Nakano, K.; Kasuga, K.; Mikuriya, M.; Matsumoto, N.; Kodera, M.; Kida, S. *Bull. Chem. Soc. Jpn.* **1992**, *65*, 3241–3252.

(46) Lindgren, T.; Sillanpää, R.; Rissanen, K.; Thompson, L. K.; O'Connor, C. J.; van Albada, G. A.; Reedijk, J. *Inorg. Chim. Acta* **1990**, *171*, 95–102.

(47) Matsumoto, N.; Tsutsumi, T.; Ohyoshi, A.; Ōkawa, H. *Bull. Chem. Soc. Jpn.* **1983**, *56*, 1388–1392.

(48) Matuzenko, G. S.; Simonov, Y. A.; Dvorkin, A. A.; Yablokov, Y. V.; Voronkova, V. K.; Mosina, L. V.; Kuyavskaya, B. Y.; Yampolskaya, M. A.; Gerbeleu, N. V. *Zh. Neorg. Khim.* **1984**, *29*, 978–986.

(49) Mikuriya, M.; Ōkawa, H.; Kida, S. *Bull. Chem. Soc. Jpn.* **1982**, *55*, 1086–1091.

(50) Mikuriya, M.; Harada, T.; Ōkawa, H.; Kida, S. *Inorg. Chim. Acta* **1983**, *75*, 1–7.

(51) Mikuriya, M.; Toriumi, K.; Ito, T.; Kida, S. *Inorg. Chim. Acta* **1985**, *24*, 629–631.

(52) Mikuriya, M.; Toriumi, K. *Bull. Chem. Soc. Jpn.* **1993**, *66*, 2106–2108.

(53) Mikuriya, M.; Ōkawa, H.; Kida, S. *Bull. Chem. Soc. Jpn.* **1981**, *54*, 2979–2982.

(54) Simonov, Y. A.; Yampolskaya, M. A.; Matuzenko, G. S.; Belskii, V. K.; Kuyavskaya, B. Y. *Zh. Neorg. Khim.* **1986**, *31*, 941–946.

(55) Tokii, T.; Nakashima, M.; Furukawa, T.; Muto, Y.; Lintvedt, R. L. *Chem. Lett.* **1990**, 363–366.

(56) Walz, L.; Haase, W. *J. Chem. Soc., Dalton Trans.* **1985**, 1243–1248.

(57) Walz, L.; Paulus, H.; Haase, W. *J. Chem. Soc., Dalton Trans.* **1985**, 913–920.

(58) Yampolskaya, M. A.; Dvorkin, A. A.; Simonov, Y. A.; Voronkova, V. K.; Mosina, L. V.; Yablokov, Y. V.; Turte, K. I.; Ablon, A. V.; Malinovskii, T. I. *Zh. Neorg. Khim.* **1980**, *25*, 174–179.

(59) Xie, Y.; Bu, W.; Xu, X.; Jiang, H.; Liu, Q.; Xue, Y.; Fan, Y. *Inorg. Chem. Commun.* **2001**, *4*, 558–560.

(60) Fallon, G. D.; Moubaraki, B.; Murray, K. S.; van den Bergen, A. M.; West, B. O. *Polyhedron* **1993**, *12*, 1989–2000.

(61) Wang, S.; Zheng, J.-C.; Hall, J. R.; Thompson, L. K. *Polyhedron* **1994**, *13*, 1039–1044.

(62) Merz, L.; Haase, W. *J. Chem. Soc., Dalton Trans.* **1980**, 875–879.

(63) Schwabe, L.; Haase, W. *J. Chem. Soc., Dalton Trans.* **1985**, 1909–1913.

(64) Matsumoto, N.; Ueda, I.; Nishida, Y.; Kida, S. *Bull. Chem. Soc. Jpn.* **1976**, *49*, 1308–1312.

(65) Merz, L.; Haase, W. *J. Chem. Soc., Dalton Trans.* **1978**, 1594–1598.

(66) Mergehenn, R.; Haase, W. *Acta Crystallogr.* **1977**, *B33*, 2734–2739.

(67) Ruiz, E.; Rodríguez-Fortea, A.; Alemany, P.; Alvarez, S. *Polyhedron* **2001**, *20*, 1323–1327.

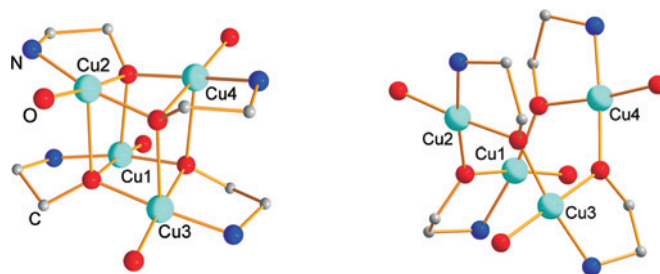


**Figure 3.** Representation of the central  $\text{Cu}_4\text{O}_4$  cores of complex **4** (left) and  $[\text{Cu}(\text{L}')_4]^{34}$  (right). All atoms except those coordinated to copper and the carbon atoms of the carbohydrate backbone chelate rings are omitted for clarity.

extreme types of core structures, there are rare intermediate cases where the  $\text{Cu}\cdots\text{Cu}$  distances tend to become equal, which have been named 6 + 0 cubanes.<sup>10</sup>

The  $\text{Cu}_4\text{O}_4$  core structure of **4** can be classified as a 2 + 4 system with two short  $\text{Cu}\cdots\text{Cu}$  distances observed within the constituting dimeric units  $\text{Cu1Cu3}$  and  $\text{Cu2Cu4}$ . In contrast to the usually observed molecular symmetries of  $S_4$  or  $D_{2d}$  for the 2 + 4 class of heterocubanes, the molecular symmetry of complex **4** can be described as approximately  $D_2$ . The absence of any kind of mirror plane is in agreement with the fact that the constituting  $\{\text{Cu}(\text{L})\}$  building blocks contain a chiral sugar as supporting ligand. Taking the trigonal imino nitrogen atoms  $N_i$  of the supporting ligand **3** as a stereochemical descriptor for the two distinct faces of the coordination planes of the  $\{\text{Cu}(\text{L})\}$  fragments, further denoted as N-Re or N-Si face, it is possible to distinguish the relative orientation of these four building blocks with respect to the central  $\text{Cu}_4\text{O}_4$  core.

According to the approximate  $D_2$  symmetry of **4**, the dimeric units  $\text{Cu1Cu3}$  and  $\text{Cu2Cu4}$  are both assembled such that the N-Re faces of their constituting  $\{\text{Cu}(\text{L})\}$  building blocks are pointing toward the same side, which is consistent with the virtual  $C_2$  axis perpendicular to the  $\text{Cu}_4\text{O}_4$  core of the dimers. Moreover, in the assembly of the  $\text{Cu}_4\text{O}_4$  cubane structure the N-Re faces of the two constituting dimers  $\text{Cu1Cu3}$  and  $\text{Cu2Cu4}$  are pointing toward each other. Again this is consistent with the virtual  $C_2$  axis, in this case defined by the opposite midpoints of the elongated cubane faces (cf. Figure 3).

We have recently published the tetranuclear copper(II) complex  $[\text{Cu}(\text{L}')_4]$  with a similar ligand  $\text{H}_2\text{L}'$ ,<sup>34</sup> with the major difference that the hydroxy groups at C-4 and C-6 of the sugar backbone were protected as a cyclic benzylidene acetal and, therefore, not available for any kind of hydrogen bonding interactions. As a result of the consequently missing stabilization by hydrogen bonding and additional steric hindrance by the benzylidene protecting groups, no formation of dimeric  $\text{Cu}_2\text{O}_2$  units analogous to those of **4** has been observed. The four  $\{\text{Cu}(\text{L}')\}$  building blocks in this case rather assemble to a  $\text{Cu}_4\text{O}_4$  cubane-like structure which can be assigned as 4 + 2 class, with the four elongated  $\text{Cu}\cdots\text{O}$  distances already in the nonbonding range of 293–321 pm. Consequently, rather large  $\text{Cu}-\text{O}-\text{Cu}$  bridging angles in the range of 121–127° are observed. This leads to two nonbonded pairs of copper ions given by  $\text{Cu1Cu3}$  and  $\text{Cu2Cu4}$  as depicted in Figure 3.

It is interesting to note that the  $\text{Cu1Cu3}$  pair can be virtually transformed into the analogous dimer found in complex **4** by simply removing the protective groups at C-4 and twisting of the two building blocks away from the approximate  $C_2$  axis. As in **4** this would lead to a dimer unit with the N-Re faces pointing toward the  $\text{Cu}_4\text{O}_4$  core. But in contrast to complex **4**, the second pair  $\text{Cu2Cu4}$ , if transformed in the same manner, leads to a dimer unit with its N-Si faces pointing toward the  $\text{Cu}_4\text{O}_4$  core. The structure of  $[\text{Cu}(\text{L}')_4]$  is thus characterized by the relative orientation of the  $\{\text{Cu}(\text{L}')\}$  building blocks of the dimeric units  $\text{Cu1Cu3}$  and  $\text{Cu2Cu4}$  with their N-Si and N-Re face, respectively, pointing toward the virtual  $C_2$  axis.

In the crystal structure of complex **4** additional solvent molecules of crystallization are present. The methanol and acetonitrile molecules are found at only partially occupied crystallographic positions (see Experimental Section), which is consistent with the TGA measurements, whereas the two water molecules are located at fully occupied positions, as depicted in Figure 4. These water molecules are additionally linking the two dimeric units  $\text{Cu1Cu3}$  and  $\text{Cu2Cu4}$  via hydrogen bonds toward the corresponding C-4 hydroxy groups at distances in the range of 270–286 pm. The C-6 hydroxy groups of the sugar backbone dangling at the periphery of **4** are cross-linking the tetrameric complex molecules by rather strong hydrogen bonds in the range of 266–276 pm.<sup>68</sup>

This leads to the formation of hydrogen bonded layers coplanar to the (001) plane as depicted in Figure 5. Whereas the hydrogen bonded water molecules are located within the established layers, the acetonitrile molecules are found between these layers. Also the disordered methanol molecules are located within the interstice between the supramolecular layers, but hydrogen bonded to the C-6 hydroxy group O35 at the hydrogen bonding nodes linking the tetrameric complexes **4** (see Figure 4).

**Magnetic Properties.** The magnetic susceptibility  $\chi$  of a polycrystalline sample of  $[\{\text{Cu}(\text{L}')_4\}]_4 \cdot 2\text{H}_2\text{O}$  (**4**·2 $\text{H}_2\text{O}$ ) was measured in a temperature range of 2–300 K with a SQUID susceptometer with an applied field of  $H = 2$  kOe. The temperature dependence of the molar susceptibility  $\chi_M$  and its product  $\chi_M T$  is shown in Figure 6.

The molar susceptibility  $\chi_M$  continuously increases with decreasing temperature without reaching a maximum in the

(68) Plass, W.; Pohlmann, A.; Rautengarten, J. *Angew. Chem., Int. Ed.* **2001**, *40*, 4207–4210.



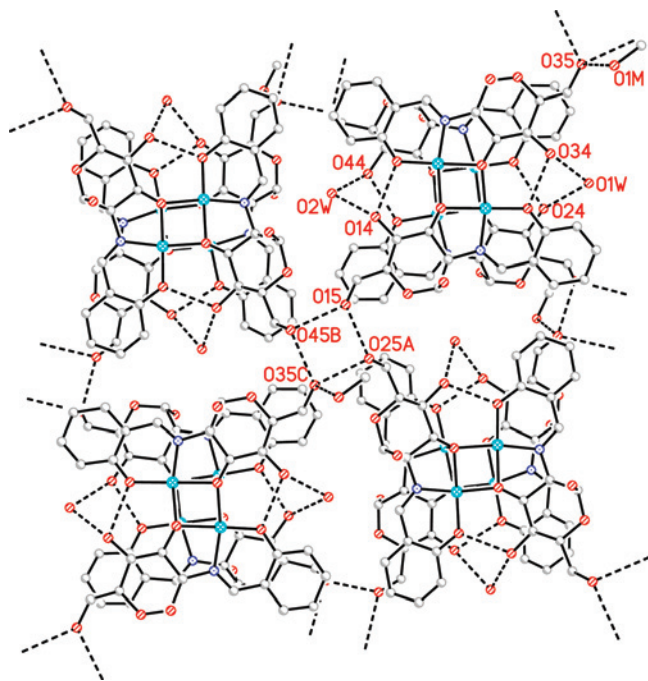


**Figure 4.** Supramolecular arrangement of complex **4** in the crystal structure of  $4 \cdot 2\text{H}_2\text{O} \cdot 0.75\text{MeOH} \cdot 2.25\text{CH}_3\text{CN}$ . Hydrogen bonds are represented as broken lines. Pertinent distances: O15...O45B 269.4(4), O15...O25A 266.6(4), O25A...O35C 276.4(4), O35C...O45B 269.7(4), O1M...O35 281.0(6), O1W...O24 278.2(4), O1W...O34 286.3(4), O2W...O14 281.4(5), O2W...O44 270.3(5) pm.

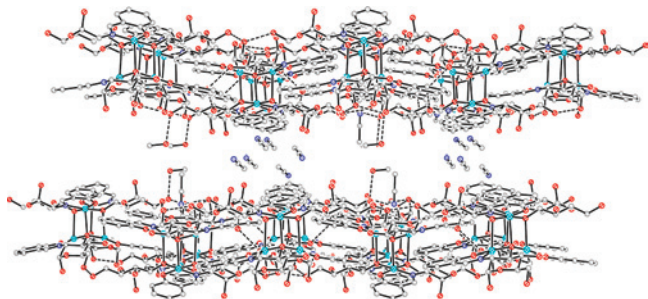


**Figure 5.** Representation of the packing in the crystal structure of  $4 \cdot 2\text{H}_2\text{O} \cdot 0.75\text{MeOH} \cdot 2.25\text{CH}_3\text{CN}$ . View approximately along [100]. Dashed lines indicate hydrogen bonds.

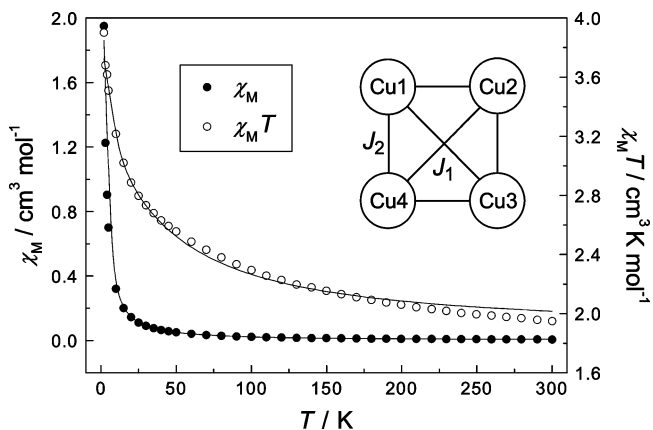


**Figure 6.** Plots of  $\chi_M$  vs  $T$  (●) and  $\chi_M T$  vs  $T$  (○) for  $[\{\text{Cu}(\text{L})\}_4] \cdot 2\text{H}_2\text{O}$  ( $4 \cdot 2\text{H}_2\text{O}$ ). The solid lines represent the best fit to the experimental data (see text).

investigated temperature range. The observed low-temperature value of  $\chi_M T$  is in accordance with an  $S = 2$  ground

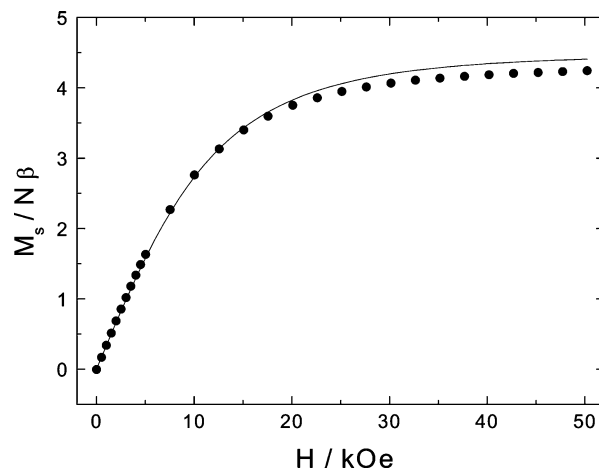


**Figure 7.** Field dependence of the magnetization for  $4 \cdot 2\text{H}_2\text{O}$  at 2 K (●). The Brillouin function for  $S = 2$  and  $g = 2.23$  is plotted as solid line.

state of complex **4**. The high-temperature value of  $1.95 \text{ cm}^3 \text{ kmol}^{-1}$  at 300 K is close to the expected spin-only value for four independent copper(II) centers. The temperature dependence of the  $\chi_M T$  product reveals ferromagnetic exchange interactions within the tetranuclear core of complex **4**.

As a result of the large intermolecular  $\text{Cu} \cdots \text{Cu}$  distances the only possible magnetic interaction is superexchange within the  $\text{Cu}_4\text{O}_4$  core via the  $\mu_3$ -bridging oxygen atoms O*i*3 (see Figure 2). Because of the similar coordinative environment of the four copper(II) centers and the  $2 + 4$  type-structure of the central  $\text{Cu}_4\text{O}_4$  core two coupling constants  $J_1$  and  $J_2$  are assumed.  $J_1$  accounts for the intradimeric exchange interaction within the Cu1Cu3 and Cu2Cu4 pairs, whereas  $J_2$  represents the coupling between the two assembled  $\text{Cu}_2\text{O}_2$  units. The Heisenberg spin Hamiltonian given in eq 1 was derived from the spin topology depicted in Figure 6.

$$\hat{H} = -J_1(\hat{S}_1\hat{S}_3 + \hat{S}_2\hat{S}_4) - J_2(\hat{S}_1 + \hat{S}_3)(\hat{S}_2 + \hat{S}_4) \quad (1)$$

Utilizing this spin Hamiltonian, the van Vleck equation leads to the expression for the magnetic susceptibility of such systems given in eq 2,<sup>2</sup> with the following abbreviations:  $A = J_1/kT$ ,  $B = (2J_1 - 2J_2)/kT$ ,  $C = (2J_1 - J_2)/kT$ , and  $D = (2J_1 + J_2)/kT$ .

$$\chi_M T = \frac{2Ng^2\beta^2}{k} \frac{2 \exp A + \exp C + 5 \exp D}{1 + 6 \exp A + \exp B + 3 \exp C + 5 \exp D} \quad (2)$$

A fit of the experimental magnetic susceptibility data of compound  $4 \cdot 2\text{H}_2\text{O}$  to the expression given in eq 2 leads the parameters  $g = 2.23$ ,  $J_1 = 64(5) \text{ cm}^{-1}$ , and  $J_2 = 4.0(3) \text{ cm}^{-1}$ , which correspond to a coefficient of determination of  $r^2 = 0.9933$  (see Figure 6). The observed ferromagnetic coupling within the  $\text{Cu}_4\text{O}_4$  core is consistent with magnetization measurements at 2 K depicted in Figure 7 which confirm a ferromagnetic  $S = 2$  ground state for complex **4**.

X-band ESR powder spectra of  $4 \cdot 2\text{H}_2\text{O}$  recorded at room temperature and at 77 K are depicted in Figure 8 and show a series of signals which can be attributed to an  $S = 2$  state

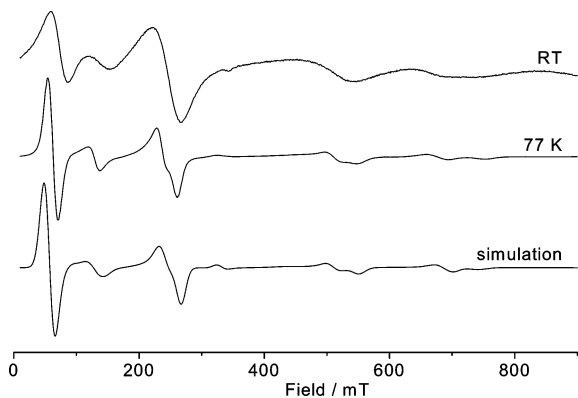


**Figure 8.** Measured and simulated polycrystalline powder ESR spectra of  $[\{\text{Cu}(\text{L})_4\} \cdot 2\text{H}_2\text{O} (4 \cdot 2\text{H}_2\text{O})$ : (top) measured at room temperature; (middle) measured at 77 K; (bottom) simulation (see text for details).

with a small zero-field splitting. The spectra were simulated<sup>69</sup> using an  $S = 2$  system at 77 K and the Hamiltonian given in eq 3, assuming that all tensors and vectors have the same principal axes and replacing  $\vec{D}$  by  $D = D_{zz} - 1/2(D_{xx} - D_{yy})$  and  $E/D = 1/2(D_{xx} - D_{yy})/D$ .

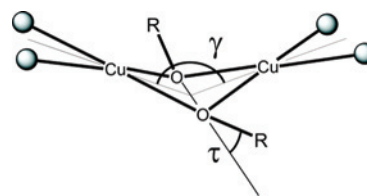
$$\hat{H} = \beta \vec{B} \hat{g} \hat{S} + \hat{S} \hat{D} \hat{S} \quad (3)$$

A good agreement between experimental and simulated spectra was obtained utilizing the following parameters:  $g_x = 2.02$ ,  $g_y = 2.02$ , and  $g_z = 2.12$  with  $D = 0.246 \text{ cm}^{-1}$  and  $E/D = 0.036$  (see Figure 8). These data are consistent with the structural features described above and represent the symmetry of a slightly distorted axial system.

For alkoxo-bridged tetranuclear copper(II) complexes with a  $2 + 4$  core structure exclusively antiferromagnetic  $S = 0$  ground states have been reported in literature.<sup>59–62</sup> Nevertheless, the two relevant coupling constants  $J_1$  and  $J_2$  show remarkable trends which can be related to geometrical parameters of the  $\text{Cu}_4\text{O}_4$  core structure. Here the  $\text{Cu}-\text{O}-\text{Cu}$  angle is of particular importance, as could be expected from the well-known magnetostructural correlations described for dinuclear copper(II) complexes with  $\text{Cu}_2\text{O}_2$  core. In these cases the  $\text{Cu}-\text{O}-\text{Cu}$  angle confines the range of ferromagnetic coupling, which is found below the limiting values of  $97.5^\circ$  ( $J = 7270 - 74.53\alpha$ ) and  $95.7^\circ$  ( $J = 7857 - 82.1\alpha$ ) for hydroxo- and alkoxo-bridged complexes, respectively.<sup>70</sup> This agrees nicely with the fact that for all relevant alkoxo-bridged tetranuclear copper(II) complexes with a  $2 + 4$  core structure  $\text{Cu}-\text{O}-\text{Cu}$  angles clearly larger than the limiting angle are observed. Interestingly, there is one report on a similar hydroxo-bridged tetranuclear copper complex with a weak ferromagnetic coupling and an angle of  $96.6^\circ$ ,<sup>71</sup> which is smaller than the confining borderline value for the corresponding dinuclear magnetostructural correlation.

The ferromagnetic coupling observed within the dimeric  $\text{Cu1Cu3}$  and  $\text{Cu2Cu4}$  units of complex **4** is in agreement with this picture, as the  $\text{Cu}-\text{O}-\text{Cu}$  bridging angles are in

**Scheme 3.** Representation of a Hinge Distorted  $\text{Cu}_2\text{O}_2$  Core (See Text)



the range of  $89.8\text{--}94.4^\circ$  (cf. Table 2), which is well below the limiting value for alkoxo-bridged dinuclear complexes. However, the coupling constant  $J_1 = 64 \text{ cm}^{-1}$  of **4** is considerably smaller than the values predicted on the basis of the relevant magnetostructural correlation, which are on the order of  $100\text{--}500 \text{ cm}^{-1}$ . Nevertheless, a recent theoretical study of Tercero et al.<sup>10</sup> on magnetostructural correlations in  $\text{Cu}_4\text{O}_4$  cubane complexes indicates that the angular dependence of the relevant coupling constant in  $2 + 4$  cubanes is considerably smaller (about 1/3) than the one observed for dinuclear alkoxo-bridged complexes.

In fact, the calculated value for an alkoxo-bridged ideal cube (all angles  $90^\circ$ ) with  $\text{Cu}-\text{O}$  distances of 200 pm was found to be ferromagnetic with about  $17 \text{ cm}^{-1}$ .<sup>10</sup> Moreover, it has been stated that the effect of increasing the interdimer distance of a  $\text{Cu}_4\text{O}_4$  cubane is twofold. First it leads to a moderate decrease of the ferromagnetic interdimer coupling constant  $J_2$  and second to a considerable increase of the antiferromagnetic nature of the intradimer coupling constant  $J_1$ . Considering the actual interdimer distances of about 250 pm in complex **4**, this would, however, predict rather weak ferromagnetic couplings for both interactions. This is consistent with the observed small ferromagnetic interdimer coupling with a value of  $J_2 = 4 \text{ cm}^{-1}$ . On the other hand, the unexpectedly large intradimer coupling constant  $J_1$ , based on the above employed distance criterion, can be understood in view of the geometrical distortions of the  $\text{Cu}_2\text{O}_2$  core of the constituting dimeric entities  $\text{Cu1Cu3}$  and  $\text{Cu2Cu4}$ .

It is well-known that a hinge distortion as depicted in Scheme 3 increases the ferromagnetic character of the relevant copper-copper coupling constant.<sup>72–76</sup> DFT calculations on dinuclear model systems indicate that a hinge distortion for a given dihedral angle  $\gamma$  of  $140^\circ$  considerably reduces the antiferromagnetic coupling (up to several hundreds of wave numbers). This effect is enhanced at about the same order of magnitude by the so-called out-of-plane distortion of the substituent on the bridging oxygen atoms at an angle of  $\tau = 35^\circ$ . Interestingly, for complex **4** similarly large distortions within the dinuclear units  $\text{Cu1Cu3}$  and  $\text{Cu2Cu4}$  are observed, with  $\gamma$  approximately  $151$  and  $160^\circ$  and  $\tau$  in the range of  $33\text{--}40^\circ$ .

(69) *XSope Computer Simulation Software Suite*, version 1.1.4; Bruker Biospin GmbH: Rheinstetten, Germany, 2004.

(70) Tuna, F.; Patron, L.; Journaux, Y.; Andruh, M.; Plass, W.; Trombe, J.-C. *J. Chem. Soc., Dalton Trans.* **1999**, 539–545.

(71) Sletten, J.; Sørensen, A.; Julve, M.; Journaux, Y. *Inorg. Chem.* **1990**, 29, 5054–5058.

(72) Lintvedt, R. L.; Glick, M. D.; Tomlonovic, B. K.; Gavel, D. P.; Kuszaj, J. M. *Inorg. Chem.* **1976**, 15, 1633–1645.

(73) Charlot, M. F.; Jeannin, S.; Jeannin, Y.; Kahn, O.; Lucrece-Abaul, J.; Martin-Frere, J. *Inorg. Chem.* **1979**, 18, 1675–1681.

(74) Charlot, M. F.; Jeannin, S.; Jeannin, Y.; Kahn, O.; Lucrece-Abaul, J.; Martin-Frere, J. *Inorg. Chem.* **1980**, 19, 1410–1411.

(75) Ruiz, E.; Alemany, P.; Alvarez, S.; Cano, J. *Inorg. Chem.* **1997**, 36, 3683–3688.

(76) Ruiz, E.; Alemany, P.; Alvarez, S.; Cano, J. *J. Am. Chem. Soc.* **1997**, 119, 1297–1303.



Clearly, the steric presettings given by the sugar backbone of the Schiff base ligand determine the ferromagnetic properties of the 2 + 4 core structure of complex **4**. Here the question arises whether this also applies for the tetranuclear copper(II) complex  $[\text{Cu}(\text{L}')_4]$  with its analogous ligand backbone (see section Structure Description).<sup>34</sup> This is of particular interest, as complex  $[\text{Cu}(\text{L}')_4]$  shows a rather large antiferromagnetic coupling constant of  $J = -130 \text{ cm}^{-1}$ , which is in contrast to the usually observed ferromagnetic coupling in 4 + 2 core structures. According to a theoretical study of Tercero et al.<sup>10</sup> it should be expected that for 4 + 2 cubane-like structures a further increase of the four already elongated  $\text{Cu}\cdots\text{O}$  distances as well as a concomitant increase in the  $\text{Cu}-\text{O}-\text{Cu}$  bridging angles will eventually lead to antiferromagnetic coupling for interactions along the short  $\text{Cu}\cdots\text{Cu}$  distances and almost vanishing interactions along the long  $\text{Cu}\cdots\text{Cu}$  distances (see Scheme 2). Given the actual values of the four elongated  $\text{Cu}\cdots\text{O}$  distances of 293–321 pm and the  $\text{Cu}-\text{O}-\text{Cu}$  bridging angles of 121–127° (cf. Figure 3), which are both considerably larger than relevant parameters in 4 + 2 cubane-like complexes with reported magnetic and structural data,<sup>10</sup> the fairly large observed antiferromagnetic coupling constant of  $J = -130 \text{ cm}^{-1}$  can be rationalized. Moreover, this also accounts for the fact that only one coupling constant has been sufficient to model the experimental data in this case.<sup>34</sup>

## Conclusions

The self-assembly of four chiral building blocks  $\{\text{Cu}(\text{L})\}$ , derived from a sugar-based Schiff base ligand, leads to the tetranuclear complex  $[\{\text{Cu}(\text{L})\}_4]$  (**4**). Complex **4** consists of a cubane-like  $\text{Cu}_4\text{O}_4$  core which is substantially distorted based on the geometric prerequisites given by the stereochemistry of the sugar-based ligand. The two constituting dimeric  $[\{\text{Cu}(\text{L})\}_2]$  units with a  $\text{Cu}_2\text{O}_2$  core are stabilized by hydrogen bonding. **4** exhibits an approximate  $D_2$  symmetry with a homochiral assembly in the solid state. Temperature dependent magnetic studies and ESR experiments reveal that complex **4** is the first alkoxo-bridged tetranuclear copper(II) complex with  $\text{Cu}_4\text{O}_4$  core representing

the 2 + 4 cubane class with ferromagnetic ground state. Moreover, **4** contains a chiral ligand backbone with its chirality transferred to the copper(II) centers and, therefore, represents a rare example for the class of molecules combining a ferromagnetic ground-state with optical activity. Superexchange via the  $\mu_3$ -oxygen atoms affords an unusual strong ferromagnetic intradimer coupling of  $J_1 = 64 \text{ cm}^{-1}$  which is attributed to the small  $\text{Cu}-\text{O}-\text{Cu}$  bridging angles and the hinge distortion within the  $\text{Cu}_2\text{O}_2$  core of the constituting dimeric units, whereas the weak interdimer coupling of  $J_2 = 4 \text{ cm}^{-1}$  is in accordance with the long  $\text{Cu}-\text{O}$  bonds between the dimeric units.

The tetranuclear copper(II) complex  $[\text{Cu}(\text{L}')_4]$  with the 4,6-benzylidene protected homologous ligand ( $\text{L}'$ ) possesses a  $\text{Cu}_4\text{O}_4$  core with 4 + 2 cubane-like structure and exceedingly large  $\text{Cu}-\text{O}-\text{Cu}$  bridging angles, as compared to other examples of this class. Together with the longest axial  $\text{Cu}-\text{O}$  distances found for 4 + 2 structures, the large  $\text{Cu}-\text{O}-\text{Cu}$  angles are responsible for the rather strong antiferromagnetic coupling of  $J = -130 \text{ cm}^{-1}$  in  $[\text{Cu}(\text{L}')_4]$ , which as yet is the largest observed for complexes of the 4 + 2 class.

The presented results show that supporting ligands with a 2-aminoglucose backbone allow the appropriate steric presettings for the assembly of alkoxo-bridged tetranuclear copper(II) complexes with  $\text{Cu}_4\text{O}_4$  core to be introduced leading to exceptional magnetic properties. In fact, complex **4** and its homologous complex  $[\text{Cu}(\text{L}')_4]$  exhibit magnetic behavior opposite to what is generally observed for 2 + 4 and 4 + 2 cubane-like complexes, respectively.

**Acknowledgment.** This work was supported by the Deutsche Forschungsgemeinschaft (SFB 436 “Metal Mediated Reactions Modeled after Nature” and SPP 1137 “Molecular Magnetism”). E.T.S. is grateful to the Freistaat Thüringen and the Carl-Zeiss-Stiftung for a Ph.D. scholarship.

**Supporting Information Available:** Experimental details for the crystallographic study in CIF format. This material is available free of charge via the Internet at <http://pubs.acs.org>.

IC701777T